第 34 卷第 10 期 无 机 化 学 学 报 Vol.34 No.10
2018 年 10 月 CHINESE JOURNAL OF INORGANIC CHEMISTRY 1936-1942

两个基于 π-共轭二羧酸构筑的配位聚合物的晶体结构、磁性及光催化性能

翟丽军*,[1] 牛宇岚[1] 郝小艳[1] 陈立杰[1] 李国放[1] 范黎明*,[2]
([1]太原工业学院化学与化工系,太原 030008)
([2]中北大学理学院,太原 030051)

摘要:在水热条件下,利用具有 π 共轭体系的二羧酸 H_2L 与金属盐进行配位反应得到 2 个新颖的配位聚合物:$\{[Mn_2(L)_2(H_2O)_5]\cdot 2H_2O\}_n$ (**1**)和$[Cd(L)(H_2O)_2]_n$ (**2**),并通过元素分析、红外光谱、粉末 X 射线衍射分析、单晶 X 射线衍射等对其结构进行了表征。结构分析表明,配合物 **1** 是具有一维$\{Mn_3(COO)_2\}$链的二维层状结构,而配合物 **2** 中镉离子与 L^{2-}配体中的羧基氧螯合配位,最终得到一维链状结构。配合物 **1** 和 **2** 都通过结构单元之间的氢键作用,最终形成三维超分子结构。此外,还研究了配合物 **1** 的磁性和配合物 **2** 的光催化活性。

关键词:配位聚合物;晶体结构;磁性;光催化
中图分类号:O614.71+1;O614.24+2 **文献标识码**:A **文章编号**:1001-4861(2018)10-1936-07
DOI:10.11862/CJIC.2018.242

Crystal Structures, Magnetic Property, and Photocatalytic Activity of Two Coordination Polymers Based on π-Conjugated Benzenedicarboxylic Acid

ZHAI Li-Jun*,[1] NIU Lan-Yu[1] HAO Xiao-Yan[1] CHEN Li-Jie[1] LI Guo-Fang[1] FAN Li-Ming*,[2]
([1]*Department of Chemistry and Chemical Engineering, Taiyuan Institute of Technology, Taiyuan* 030008, *China*)
([2]*Department of Chemistry, College of Science, North University of China, Taiyuan* 030051, *China*)

Abstract: Two coordination polymers, namely $\{[Mn_2(L)_2(H_2O)_5]\cdot 2H_2O\}_n$ (**1**) and $[Cd(L)(H_2O)_2]_n$ (**2**), have been assembled from the π-conjugated ligand of 3,3′-(1,3,6,8-tetraoxobenzol[lmn][3,8]-phenanthroline-2,7(1*H*,3*H*,6*H*,8*H*)diyl)-di-benzoic acid (H_2L) under hydrothermal condition. Their structures have been determined by single-crystal X-ray diffraction analyses and further characterized by elemental analyses (EA), IR spectra, powder X-ray diffraction (PXRD), and thermogravimetric (TG) analyses. Structural analysis reveals that complex **1** is a 2D sheet with 1D $\{Mn_3(COO)_2\}$ chain, which was further expanded to a 3D supramolecular structure through hydrogen bonds. While complex **2** is a 1D polymeric chain, which can be packed into a 3D supramolecular through hydrogen bonding interactions. Besides, the variable-temperature susceptibility of **1** as well as the photocatalytic activity of **2** have been investigated. CCDC: 1848147, **1**; 1848148, **2**.

Keywords: coordination polymers; crystal structure; magentic property; photocatalytic activity

Coordination polymers (CPs), have attracted more and more attentions of chemists and materials scientist for their widely applications as functional materials[1-4]. Generally speaking, the CPs are assembled from organic linkers and inorganic nodes[5-6]. It is well known that the physicochemical properties of CPs are

收稿日期:2018-07-07。收修改稿日期:2018-08-13。
国家自然科学基金(No.21676258)资助项目。
*通信联系人。E-mail:jinzhongzhailijun@163.com,limingfan@nuc.edu.cn

greatly depending on the nature of the organic ligands. Thus, the rational selection of organic linkers plays important roles in the design of targeting CPs[7-9].

Numberous organic ligands have been introduced into the construction of CPs in the recent three decades. Among them, there was no doubt the polycarboxylates are still dominant for their strong coordinating abilities, diverse coordination modes, stable backbones[10-11]. It is noteworthy that the π-conjugated polycarboxylates based CPs exhibits interesting single-chain magnet and luminescent properties for their unique π-conjugated system[12]. At the same time, the π-conjugated polycarboxylates based CPs are rarely reported up to now[13]. Thus, the design of π-conjugated polycarboxylates based CPs is meaningful.

Inspired by above mentioned points, we explored novel CPs based on the π-conjugated ligand of 3,3′-(1, 3, 6, 8-tetraoxobenzol[lmn][3,8]-phenanthroline-2,7(1*H*,3*H*,6*H*,8*H*) diyl)-di-benzoic acid) (H_2L, Scheme 1). Herein, we reported the structure and characterizations of two CPs, $\{[Mn_2(L)_2(H_2O)_5]\cdot 2H_2O\}_n$ (**1**) and $[Cd(L)(H_2O)_2]_n$ (**2**), which displaying 2D sheet with 1D $\{Mn_3(COO)_2\}$ SBUs for **1**, and 1D polymeric chain for **2**, respectively. Expanded by hydrogen bonds, both two CPs show 3D supramolecular finally. Besides, the magnetic property of **1** as well as the photocatalytic activity of **2** have been investigated.

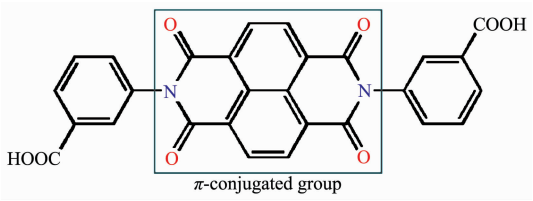

Scheme 1　Structure of H_2L

1　Experimental

1.1　Materials and methods

All the chemical reagents were purchased from Jinan Henghua Sci. & Technol. Co., Ltd. without further purification. IR spectra were measured on a NEXUS 670 FTIR spectrometer. Elemental analyses were carried out on a CE instruments EA 1110 elemental analyzer. Thermogravimetric analyses (TGA) were performed with a heating rate of 10 ℃·min^{-1} under N_2 atmosphere on Perkin-Elmer TGA-7 thermogravimetric analyzer. Powder X-ray diffraction (PXRD) determinations were performed on an X-ray diffractometer (D/max 2500 PC, Rigaku) at 50 kV, 30 mA by using Cu *Kα* radiation (λ=0.154 06 nm) with the 2θ range of 5°~50°. The variable-temperature magnetic susceptibility measurements were performed on the Quantum Design SQUID MPMS XL-7 instruments. Photocatalytic experiments were evaluated by the degradation of methylene blue (MB) under UV light irradiation using a 300 W metal-halide lamp as the light source. 0.5 mL of 30%(*w*/*w*) hydrogen peroxide was injected into 20.0 mL 10 mg·L^{-1} methylene blue (MB) aqueous solution with 10 mg powdered catalyst (30 min dark adsorption pretreated). During the degradation, the reaction solution was sampled at specific time-points and centrifuged to remove the photocatalysts in order to monitor the absorption curves of MB (500~700 nm) by using a Hitachi U-3500 UV-Vis spectrometer.

1.2　Synthesis

1.2.1　Synthesis of $\{[Mn_2(L)_2(H_2O)_5]\cdot 2H_2O\}_n$ (**1**)

A mixture of H_2L (0.005 mmol, 2.5 mg), $MnCl_2\cdot 4H_2O$ (0.010 mmol, 2.0 mg), a drop of 0.5 mol·L^{-1} NaOH aqueous solution, and 1 mL H_2O was sealed in a pressure-resistant glass tube and heated at 130 ℃ for 3 days, and then cooled to room temperature at a descent rate of 5 ℃·h^{-1}. The colorless block crystals of **1** were obtained with the yield of about 37% based on H_2L. Anal. Calcd. for $C_{56}H_{38}Mn_2N_4O_{23}$(%): C, 54.03; H, 3.08; N, 4.50. Found (%): C, 54.43; H, 3.12; N, 4.56. IR (KBr, cm^{-1}): 3 337 (m), 2 367 (m), 1 715 (s), 1 674 (vs), 1 559 (vs), 1 403 (s), 1 348 (s), 1 254 (s), 1 199 (m), 1 125 (w), 983 (m), 901 (w), 772 (m), 738 (s), 684 (m), 623 (w), 575 (w).

1.2.2　Synthesis of $[Cd(L)(H_2O)_2]_n$ (**2**)

A mixture of H_2L (0.005 mmol, 2.5 mg), and $CdCl_2\cdot 2.5H_2O$ (0.010 mmol, 2.3 mg), and 1 mL H_2O was sealed in a pressure-resistant glass tube and heated at 130 ℃ for 3 days, and then cooled to room temperature at a descent rate of 5 ℃·h^{-1}. The orange block crystals of **2** were obtained with the yield of about 45% based on H_2L. Anal. Calcd. for $C_{28}H_{16}CdN_2O_{10}$

(%): C, 51.51; H, 2.47; N, 4.29. Found (%): C, 51.53; H, 2.51; N, 4.28. IR (KBr, cm^{-1}): 3 317 (m), 2 360 (m), 1 716 (vs), 1 669 (vs), 1 539 (s), 1 442 (m), 1 405 (s), 1 350 (vs), 1 253 (s), 1 198 (s), 1 117 (m), 980 (m), 887 (m), 840 (w), 768 (m), 736 (m), 686 (m), 628 (m), 553 (w).

1.3 X-ray crystallography

Structural integrity single crystals of **1** and **2** were carefully selected under an optical microscope and fixed to thin glass fibers. After that, single-crystal X-ray diffraction analyses were performed on a Siemens SMART diffractometer using Mo $K\alpha$ radiation (λ = 0.071 073 nm) at 200(2) K for **1**, and 295(2) K for **2**, respectively. The structures of two obtained CPs were solved by direct methods, with the non-hydrogen atoms refined anisotropially by using the SHELXTL package with F^2 values based full-matrix least-squares procedure[14]. All the hydrogen atoms except those for water molecules were generated geometrically with fixed isotropic thermal parameters, and included in the structure factor calculations[15]. And the hydrogen atoms attached to oxygen were refined with O-H 0.085 nm and $U_{iso}(H)=1.2U_{eq}(O)$. The crystallographic data and the details of the crystal structures are listed in Table 1. Selected bond lengths and angles for complexes **1** and **2** are listed in Table S1.

CCDC: 1848147, **1**; 1848148, **2**.

Table 1 Crystal structure parameters of complexes 1 and 2

	1	2
Empirical formula	$C_{56}H_{38}Mn_2N_4O_{23}$	$C_{28}H_{16}CdN_2O_{10}$
Formula weight	1 244.78	652.83
Crystal system	Triclinic	Monoclinic
Space group	$P\bar{1}$	$C2/c$
a / nm	0.873 62(3)	3.925 49(16)
b / nm	1.557 22(5)	0.515 44(2)
c / nm	1.943 96(6)	1.224 51(5)
α / (°)	108.161(3)	
β / (°)	93.905(3)	105.082(4)
γ / (°)	90.731(3)	
V / nm^3	2.505 41(15)	2.392 27(17)
Z	2	4
D_c / ($g\cdot cm^{-3}$)	1.650	1.813
F(000)	1 272	1 304
μ(Mo $K\alpha$) / mm^{-1}	0.601	0.983
Index ranges (h, k, l)	−10~10, −19~19, −24~24	−52~52, −7~7, −15~16
θ range for data collection / (°)	2.95~26.37	3.225~29.613
Reflection collected, unique	36 730, 10 220	16 972, 3 007
Refinement method	Full-matrix least-squares on F^2	
Goodness-of-fit on F^2	0.982	1.138
R_1, wR_2 [$I>2\sigma(I)$]	0.053 8, 0.095 8	0.025 4, 0.059 6
R_1, wR_2 (all data)	0.110 2, 0.115 5	0.030 9, 0.062 9
R_{int}	0.084 4	0.030 8

2 Results and discussion

2.1 Crystal structure of $\{[Mn_2(L)_2(H_2O)_5]\cdot 2H_2O\}_n$ (1)

X-ray crystallography reveals that complex **1** crystallizes in the triclinic system, space group $P\bar{1}$. As shown in Fig.1, the asymmetric unit consists of two Mn(Ⅱ) ions, two L^{2-} ligands, five coordinated water molecules, and two lattice water molecules. Mn (1) is located in a distorted {MnO_6} octahedral geometry,

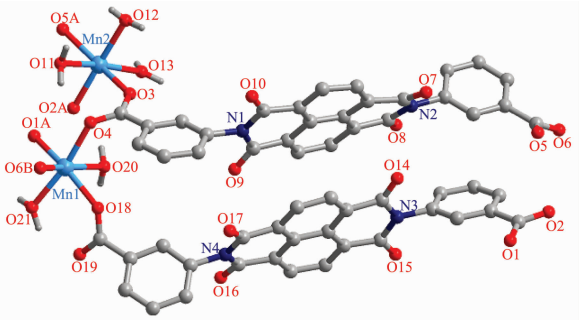

Symmetry codes: A: x, y, $-1+z$; B: $-1+x$, y, $-1+z$

Fig.1　Asymmetric unit of **1**

completed by four carboxyl O atoms (O4, O18, O1A and O6B) from four distinct L^{2-} ligands, and two water molecules (O20 and O21). Mn(2) lies in the center of a similar $\{MnO_6\}$ octahedral geometry, surrounded by three carboxyl O atoms (O3, O2A and O5A) from three L^{2-} ligands, and three coordinated water molecules (O11, O12 and O13). Besides, the Mn-O bond lengths are in the range of 0.212 6(2)~0.228 3(7) nm.

In the assembly of complex **1**, the H_2L ligands are completely deprotonated and adopts two different kinds of coordination modes: $(\kappa^1\text{-}\kappa^0)\text{-}(\kappa^1\text{-}\kappa^1)\text{-}\mu_3$ (Mode Ⅰ, Scheme 2) with the dihedral angles of α_1, β_1 and γ_1 being 57.29°, 86.26° and 37.22° (α_1, β_1, γ_1 corresponding to the dihedral angles between the aromatic functional groups of A/B, B/C and A/C), and $(\kappa^1\text{-}\kappa^1)\text{-}(\kappa^1\text{-}\kappa^1)\text{-}\mu_4$ (Mode Ⅱ, Scheme 2) with the dihedral angles of being 75.57°, 56.60° and 18.98°. It is noteworthy that the $\mu_2\text{-}\eta^1\text{:}\eta^1$ carboxyl groups of two kinds L^{2-} ligands bridged Mn(Ⅱ) ions to form an infinite 1D $\{Mn_3(COO)_2\}$ chain with the nearest Mn⋯Mn distances being 0.458 8 nm and 0.503 3 nm, respectively (Fig.2, and Fig. S1). The L^{2-} ligands act as pillars to bridge the 1D $\{Mn_3(COO)_2\}$ chains, finally leaving a 2D sheet (Fig.3). Adjacent sheets interact with each other or guest water molecules through O–H⋯O hydrogen bonds (Table S2), finally giving a 3D supramolecular structure (Fig.S2). Among them, the lattice water molecules cooperate with the coordinated water molecules through O–H⋯O hydrogen bonding interactions, forming an interesting water cluster (Fig. S3).

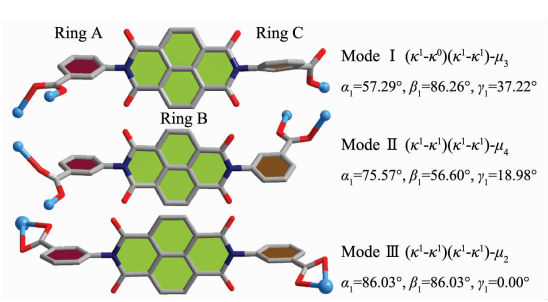

Scheme 2　Coordination modes of H_2L in complexes **1** and **2**

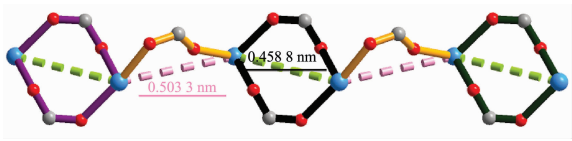

Fig.2　One dimensional $\{Mn_3(COO)_2\}$ chain in **1**

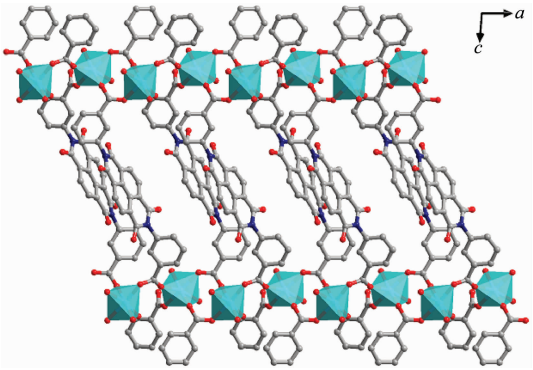

Fig.3　Two dimensional sheet of complex **1** views along b axis

2.2　Crystal structure of $[Cd(L)(H_2O)_2]_n$ (2)

Complex **2** crystallizes in the monoclinic system $C2/c$ and the structure contains a half of Cd(Ⅱ) ions, a half of L^{2-} ligands, and one coordinated water molecule (Fig.4). The central Cd(Ⅱ) ion is located in distorted $\{CdO_6\}$ triangular prism coordination geometry, surrounded by four carboxyl oxygen atoms from two L^{2-} ligands (O1, O2, O1A and O2A), and two coordinated water molecules (O1W and O1WA). And the Cd-O bond distances range from 0.220 3(9) to 0.251 5(5) nm.

Different from that in complex **1**, the H_2L ligand

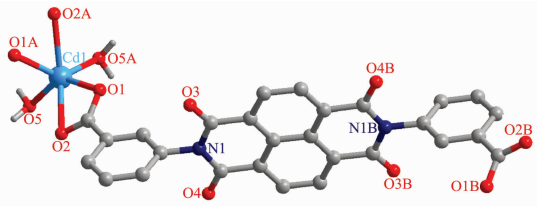

Symmetry codes: A: $1-x$, y, $1/2-z$; B: $1-x$, $1-y$, $-z$

Fig.4　Asymmetric unit of **2**

adopts (κ^1-κ^1)-(κ^1-κ^1)-μ_2 (Mode Ⅲ, Scheme 2, with α_1, β_1 and γ_1 being 86.03°, 86.03° and 0.00°) coordination mode to bridge two Cd(Ⅱ) ions by using the chelating η^2 carboxyl groups, leaving a 1D chain with the neighbouring Cd…Cd distance of 2.029 5 nm (Fig.5). Expanded by the O–H…O hydrogen bonds along *b* axis, a 2D sheet is constructed (Fig.S4). Those 2D sheets interact with adjacent ones through C/O–H…O hydrogen bonds (Table S2), finally giving a 3D supramolecular structure(Fig.S5).

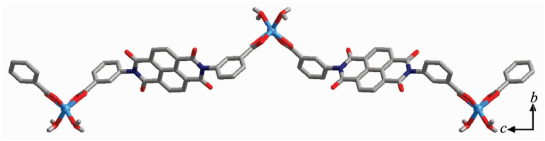

Fig.5 One dimensional polymeric chain structure of **2** view along *a* axis

2.3 Structural comparison

Up to now, only one CP based on 3,3′-(1,3,6,8-tetraoxobenzol[lmn][3,8]-phenanthroline-2,7(1*H*,3*H*,6*H*,8*H*)diyl)-di-benzoic acid) (H_2L), namely, NKUMOM-3[14], has been reported. We designed two novel CPs here and compared those structures. As can be seen in the Scheme 2, the L^{2-} adopted two different coor-dination modes: (κ^1-κ^0)-(κ^1-κ^1)-μ_3 (Mode Ⅰ) and (κ^1-κ^1)-(κ^1-κ^1)-μ_4 (Mode Ⅱ) in **1**, (κ^1-κ^1)-(κ^1-κ^1)-μ_2 (Mode Ⅲ) in **2**, and (κ^1-κ^0)-(κ^1-κ^0)-μ_2 (Mode Ⅳ) in NKUMOM-3. When comparing the structures of those CPs, we can notice that the bridging μ_2-η^1 :η^1 carboxyl groups, chelating η^2 carboxyl groups, as well as the mono-dentate η^1 carboxyl groups, are crucial role in forming different architectures. And the coordinated solvent molecules also greatly affect the final structures, for their steric hindrance and bridging effects after coordinating with metal ions. Besides, although all the metal ions in above mentioned CPs are penta-coordinated with atoms from L^{2-} ligands and solvent molecules, the coordination preference of those central metal ions also adds one hand in adjusting the structure diversity.

2.4 Powder X-ray diffraction and thermogravimetric analysis

In order to check the phase purity of the complexes, the PXRD patterns were checked at room temperature. As shown in Fig.S6, the peak positions of the simulated and experimental PXRD patterns were in agreement with each other, demonstrating the good phase purity of the complexes. The dissimilarities in intensity may be due to the preferred orientation of the crystalline powder samples.

To examine the thermal stability of two CPs, the thermogravimetric analyses were carried out from ambient temperature up to 800 ℃, and the results are given in Fig.6. For complex **1**, the first weight loss of 2.91% before 85 ℃, corresponds to the loss of lattice water molecules (Calcd. 2.89%), then the release of coordinated water molecules (Found: 7.17%; Calcd. 7.23%) occurred in the temperature range of 85~195 ℃. The architecture can exist stably until the temperature up to 450 ℃. For complex **2**, the first weight loss of 5.37% before 180 ℃, corresponds to the release of coordinated water molecules (Calcd. 5.51%). Beyond 435 ℃, there was a rapid weight loss, suggesting the decomposition of complex **2**. Both two TG curves show the high thermal stabilities of two complexes, which is important for the CPs as functional material in practical application.

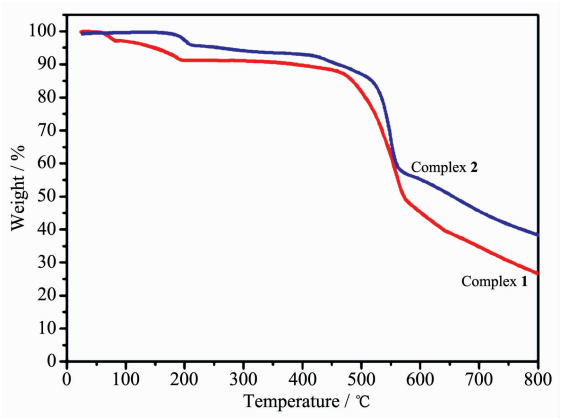

Fig.6 TG curves of complexes **1** and **2**

2.5 Magnetic property

Variable-temperature susceptibility of complex **1** was measured in the temperature range of 2~300 K with an applied magnetic field of 1 000 Oe. For complex **1**, the $\chi_M T$ value at room temperature are 7.72 $cm^3 \cdot K \cdot mol^{-1}$ (Fig.7), smaller than that for two isolated Mn(Ⅱ) cations (8.80 $cm^3 \cdot K \cdot mol^{-1}$), which can be attributed to the contribution to the susceptibility

from orbital angular momentum at higher temperatures[16]. With the temperature decreasing, the $\chi_M T$ value decreased continuously to 6.81 $cm^3 \cdot K \cdot mol^{-1}$ at 2 K. And the temperature dependence of χ_M follows the Curie-Weiss law $\chi_M = C/(T-\theta)$ with C=7.78 $cm^3 \cdot K \cdot mol^{-1}$, θ=−7.92 K (Fig.S7). The negative value of θ indicates the presence of the antiferromagnetic interactions between the Mn(Ⅱ) cations in complex **1**[17-18].

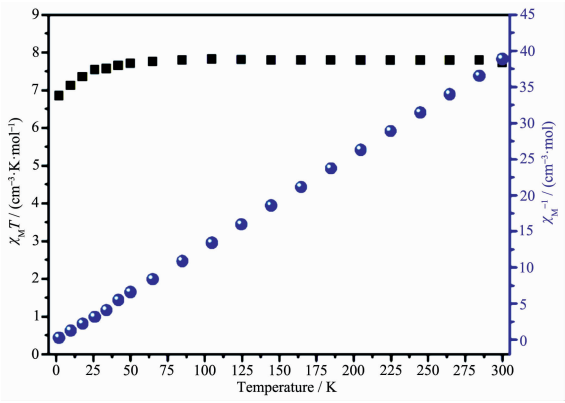

Fig.7　$\chi_M T$ and χ_M^{-1} versus T plots for complex **1**

2.6　Photocatalytic activity

The photocatalytic activity of complex **2** as photocatalyst in degradating methylene blue (MB) was investigated. The decomposition of dye MB was monitored by the characteristic absorption band at 664 nm. As illustrated in Fig.8, changes in the concentration of MB solution are plotted vs irradiation time, with the degradation efficiency of MB being 74.1% after 120 minute. Under the same conditions, the total catalytic degradation efficiency of the control experiment under illumination after 120 minute was 15.7%. The kinetic data for the degradation of MB can be well fitted by the apparent first-order reaction model, $\ln(C/C_0) = -kt$ (Fig.S8), where k is the rate constant, C_0 and C are the concentration of MB at irradiation time t=0 and t, respectively. After calculation, the rate constant value of k was found to be 0.010 7 min^{-1}.

The possible mechanism for the MB degradation is proposed as described in the previous literature[19-20]. Under the irradiation of UV-Vis light, the organic ligands are induced to produce O-Cd charge transfer promoting electrons from the highest occupied molecular orbital (HOMO) to the lowest unoccupied molecular orbital (LUMO)[21]. Therefore, the HOMO strongly needs one electron to return to its stable state. Thus, one electron is captured from water molecules, which is oxygenated to generate the ·OH radicals. And then the ·OH active species could decompose the MB effectively to complete the photocatalytic process[22].

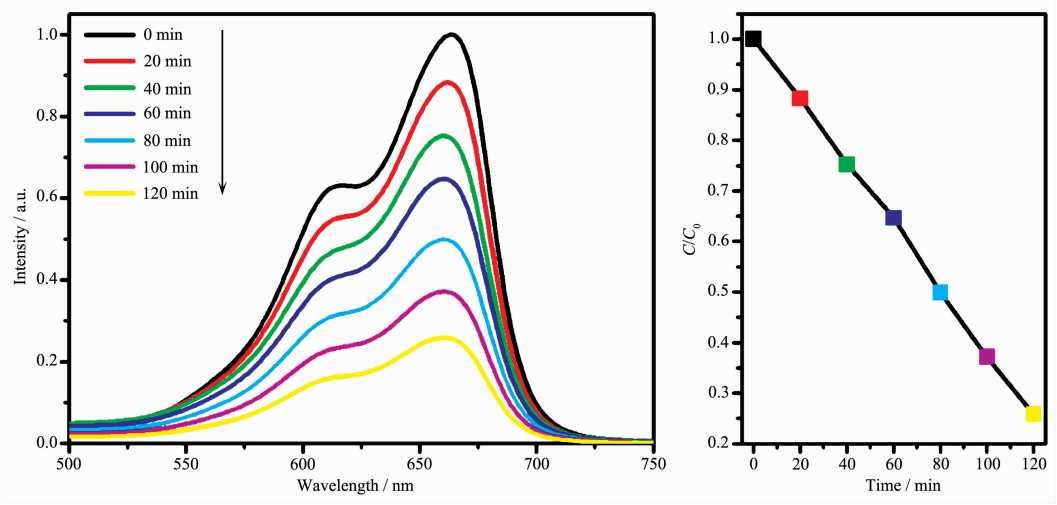

Fig.8　UV-Vis absorption spectra of the MB solutions degraded by complex **2** as photocatalyst under UV irradiation at different time intervals

3　Conclusions

In summary, two novel CPs have been constructed from the π-conjugated ligand of 3,3′-(1,3,6,8-tetraoxobenzol [lmn] [3,8]-phenanthroline-2,7 (1*H*,3*H*,6*H*,8*H*)diyl)-di-benzoic acid), with the structures being

2D sheet containing 1D $\{Mn_3(COO)_2\}$ chains for **1**, and 1D polymeric chain for **2**, respectively. With the help of hydrogen bonds, two CPs form 3D supramolecular structure finally. Thermal stability analysis revealed both two CPs show high thermal stabilities up to 450 ℃. Besides, the variable-temperature susceptibility of **1** indicated there are antiferromagnetic interactions between the Mn(Ⅱ) cations. And the photocatalytic tests demonstrated that the obtained complex **2** is good photocatalyst in the degradation of MB, with the efficiency up to 74.1% after 2 hours.

References:

[1] Zhang J P, Zhang Y B, Lin J B, et al. *Chem. Rev.*, **2012**,**112**: 1001-1033

[2] Liu Z Q, Chen K, Zhao Y, et al. *Cryst. Growth Des.*, **2018**, **18**:1136-1146

[3] Zhao D, Li X H, Guo J H, et al. *Inorg. Chem.*, **2018**,**57**:2695 -2704

[4] Lin G Q, Ding H M, Yuan D Q, et al. *J. Am. Chem. Soc.*, **2016**,**138**:3302-3305

[5] Jiang J C, Zhao Y B, Yaghi O M. *J. Am. Chem. Soc.*, **2016**, **138**:3255-3265

[6] ZHANG Xiu-Tang(张修堂), FAN Li-Ming(范黎明), SUN Zhong(孙忠), et al. *Chinese J. Inorg. Chem.*(无机化学学报), **2012**,**28**(9):1809-1816

[7] Fan L M, Fan W L, Li B, et al. *CrystEngComm*, **2015**,**17**: 9413-9422

[8] Fan W D, Wang Y T, Xiao Z Y, et al. *Inorg. Chem.*, **2017**,**56**: 13634-13637

[9] Fan L M, Zhao L, Wang J, et al. *J. Solid State Chem.*, **2018**, **266**:189-195

[10]ZHANG Qi-Long(张奇龙), WANG Huan-Yu(王焕宇), JIANG Feng(江峰), et al. *Chinese J. Inorg. Chem.*(无机化学学报), **2016**,**32**(3):464-468

[11]Fan L M, Zhang Y J, Wang J, et al. *J. Solid State Chem.*, **2018**,**260**:46-51

[12]Ren G H, Gao L L, Wang X Q, et al. *Inorg. Chim. Acta*, **2018**,**471**:746-753

[13]Ma X Z, Zhang Z J, Shi W, et al. *Chem. Commun.*, **2014**,**50**: 6340-6342

[14]Sheldrick G M. *SADABS, Version* 2.05, University of Göttingen, Germany, **1996**.

[15]Sheldrick G M. *SHELXS*-97, *Program for Crystal Structure Refinement*, University of Göttingen, Germany, **1997**.

[16]Kahn O. *Molecular Magnetism*. New York: Wiley-VCH, **1993**.

[17]Fan L M, Fan W L, Li B, et al. *Dalton Trans.*, **2015**,**44**:2380 -2389

[18]Fan L M, Wang X Q, Zhang Y J, et al. *Z. Anorg. Allg. Chem.*, **2017**,**643**:2138-2143

[19]ZHANG Qi-Long(张奇龙), FENG Guang-Wei(冯广卫), HU Peng(胡鹏). *Chinese J. Inorg. Chem.*(无机化学学报), **2014**, **30**(10):2433-2439

[20]Cui J W, Hou S X, Li Y H, et al. *Dalton Trans.*, **2017**,**46**: 16911-16924

[21]Shi W J, Du L Y, Yang H Y, et al. *Inorg. Chem.*, **2017**,**56**: 10090-10098

[22]Jia L Y, Chen N N, Luo Q, et al. *J. Mol. Struct.*, **2017**,**1149**: 596-601